Published in final edited form as:
Biol Blood Marrow Transplant. 2014 May ; 20(5): 705–716. doi:10.1016/j.bbmt.2014.01.032.

Engineering Human Peripheral Blood Stem Cell Grafts That Are Depleted of Naïve T Cells and Retain Functional Pathogen-Specific Memory T cells

Marie Bleakley, BMBS, PhD[1,2], **Shelly Heimfeld, PhD**[1], **Lori A. Jones, PhD**[3], **Cameron Turtle, MBBS PhD**[1,4], **Stanley R. Riddell, MD**[1,4,*], and **Warren Shlomchik, MD**[5,*]

[1]Fred Hutchinson Cancer Research Center, Seattle, WA

[2]Department of Pediatrics, University of Washington, Seattle, WA

[3]Seattle Cancer Care Alliance, Seattle, WA

[4]Department of Medicine, University of Washington, Seattle, WA

[5]Yale University School of Medicine, New Haven, CT

Abstract

Graft-versus-host disease (GVHD) is a frequent major complication of allogeneic hematopoietic cell transplantation (HCT). The development of approaches that selectively deplete T cells that cause GVHD from allogeneic stem cell grafts and preserve T cells specific for pathogens may improve HCT outcomes. It has been hypothesized that the majority of T cells that can cause GVHD reside within the naïve T cell (T_N) subset, and previous studies performed in mouse models and with human cells *in vitro* support this hypothesis. As a prelude to translating these findings to the clinic, we developed and evaluated a novel, two-step, clinically compliant procedure for manipulating peripheral blood stem cells (PBSC) to remove T_N, preserve $CD34^+$ hematopoietic stem cells, and provide for a fixed dose of memory T cells (T_M) that includes T cells with specificity for common opportunistic pathogens encountered after HCT. Our studies demonstrate effective and reproducible performance of the immunomagnetic cell selection procedure for depleting T_N. Moreover, after cell processing the CD45RA-depleted PBSC products are enriched for $CD4^+$ and $CD8^+$ T_M with a central memory phenotype and contain T_M cells that are capable of proliferating and producing effector cytokines in response to opportunistic pathogens.

Corresponding author: Marie Bleakley, Program in Immunology, Clinical Research Division, Fred Hutchinson Cancer Research Center, 1100 Fairview Ave Nth., Seattle, WA, 98109, Phone: 206 667 6572, Fax: 206 667 7983, mbleakle@fhcrc.org.
*Co-senior authors

Conflicts of interest: The authors declare no competing financial interests.

Introduction

Graft-versus-host disease (GVHD) is a frequent cause of morbidity and mortality after allogeneic hematopoietic cell transplantation (HCT) due to direct organ damage, and to opportunistic infections that result from immunosuppressive therapies (1). In human leukocyte antigen (HLA)-identical HCT, GVHD results from recognition of minor histocompatibility (H) antigens expressed on recipient tissues by donor T cells (1–4). Prophylactic immunosuppressive drugs are commonly administered early after HCT to suppress alloreactive T cells, however the incidence of grade II–IV acute GVHD and extensive chronic GVHD following peripheral blood stem cell transplant (PBSCT) from HLA-matched sibling donors remains unacceptably high at 40–80% and 40–50% respectively (5–8). Complete T cell depletion (TCD) of donor hematopoietic cell products is highly effective for preventing GVHD, but is complicated by a profound delay in immune reconstitution, which contributes to life threatening infections (9–20). Thus, the development of approaches that preferentially deplete from allogeneic stem cell grafts the T cells that primarily cause GVHD and preserve T cells specific for pathogens may improve HCT outcomes.

Mature $CD3^+CD8^+$ and $CD3^+CD4^+$ T cells can be broadly classified into $CD45RA^+CD62L^+$ naïve (T_N) and $CD45RO^+$ memory (T_M) subsets, the latter of which includes effector memory (T_{EM}) and central memory (T_{CM}) T cells. T_N and T_M differ in cell surface phenotype, prior exposure to cognate antigen, functional activity, and transcriptional programs (21–27). It has been hypothesized that the majority of T cells that can respond to minor H antigens and cause GVHD reside within the T_N subset, unless the donor has developed a T_M response through exposure to allogeneic cells by pregnancy or blood transfusion (4). Murine studies wherein the potency of T_N and T_M to induce GVHD has been compared support this hypothesis. In mouse models, T_N cause severe GVHD, whereas T_{CM} cause no or mild GVHD and T_{EM} do not cause GVHD (28–37). *In vitro* studies performed with human T cells have demonstrated that donor $CD8^+$ T cells specific for recipient minor H antigens are found predominantly within the T_N subset, suggesting that selective depletion of this subset may reduce the incidence or severity of GVHD in human HCT (38). Here we describe a clinically compliant process for effectively engineering human PBSC grafts that are extensively depleted of $CD45RA^+$ T_N but retain both $CD34^+$ hematopoietic stem cells and functional T_M specific for a broad range of opportunistic pathogens. This strategy for preparing PBSC products is currently being evaluated in a clinical trial.

Materials and Methods

Human subjects

Cell selection procedures were performed on granulocyte colony stimulating factor (GCSF) mobilized peripheral blood stem cell products (G-PBSC) obtained from an initial cohort of HCT donors participating in a clinical trial of T_N depletion being conducted at Fred Hutchinson Cancer Research Center (FHCRC) and Yale University School of Medicine (YUSM) under a Food and Drug Administration (FDA) Investigational Device Exemption (IDE). The Institutional Review Boards (IRB) of the FHCRC and YUSM approved the

clinical trial, and the related HCT donors and recipients provided informed written consent in accordance with the Declaration of Helsinki. Full details of the trial protocol and clinical outcomes will be described in a subsequent publication upon completion of enrollment and data analysis. HCT donors and recipients consented to providing an aliquot of the starting G-PBSC and CD45RA-depleted G-PBSC products to evaluate the cellular composition of the graft and the presence of T cell responses to pathogen-derived antigens. Blood samples and G-PBSC were also obtained from normal volunteer and HCT donors who participated in research protocols approved by the IRB of FHCRC to develop the cell selection procedures, and provided written consent in accordance with the Declaration of Helsinki.

Cell processing

A two-step cell processing procedure that involved selection of $CD34^+$ cells followed by depletion of $CD45RA^+$ cells was performed on G-PBSC apheresis products using the CliniMACs instrument (Miltenyi Biotec GmbH, Bergisch Gladbach, Germany). $CD34^+$ selections were performed using the CliniMACS CD34 reagent system (20, 39). A GMP-grade murine αCD45RA mAb (clone T6D11) directly conjugated to Miltenyi iron dextran beads was produced by Miltenyi Biotec under contract from the NIH RAID (Rapid Access to Intervention Development) program and used for depletion of $CD45RA^+$ cells from the $CD34^-$ fraction. In brief, processing involved the following steps: G-PBSC apheresis products were obtained from donors, sampled and stored overnight at 4°C prior to processing. If the cell concentration of the product was greater than 200×10^6 cells/mL, the volume was increased by the addition of 1% human serum albumin (HSA)/Normosol-R to reduce the cell concentration to ≤ 200 $x10^6$ cells/ml. The total nucleated cell and $CD34^+$ cell numbers were used to determine whether to proceed to cell processing immediately after overnight storage or to pool the initial apheresis product with a second product collected the following day.

$CD34^+$ cell selection—We set a post-selection $CD34^+$ cell dose target of $>5.0 \times 10^6$ $CD34^+$ cells/kg because $CD34^+$ cell doses exceeding this threshold have been associated with improved overall survival in recipients of PBSC transplantation (PBSCT) (40). After overnight storage or pooling, cells were washed twice with CliniMACS PBS/EDTA buffer. Cells were then incubated on a rotator for 30 minutes with CD34-Reagent according to manufacturer's instructions. After incubation, cells were washed once and then loaded onto a CliniMACS Cell Selection instrument (CliniMACS). An LS tubing set was used for the selection regardless of the number of cells loaded. The CD34 Selection 2 program software version 2.40 was used for selection, and the resulting CD34-enriched cell population was evaluated for sterility, total nucleated cell count using a hematology analyzer, and content and viability of $CD34^+$, $CD3^+$ and $CD3^+CD45RA^+CD45RO^-$ cells using a FACSCalibur flow cytometer (BD Biosciences San Jose, CA).

$CD45RA^+$ cell depletion—We set a target $CD3^+$ T cell dose of 1×10^7 T cells/kg because this total number of T cells is 10 to 100-fold greater than the threshold dose of unselected T cells predicted to cause GVHD after HLA-identical sibling HCT (41) and approximates the dose in an unmanipulated bone marrow allograft, and would therefore be appropriate to test the hypothesis that $CD45RA^-$ T cells can be transplanted with less

GVHD. We reasoned that this total T cell dose would also provide a sufficient number of T_M cells to improve immune reconstitution as compared to recipients of a TCD allograft. We restricted the allowable number of $CD3^+CD45RO^-CD45RA^+$ T_N to $<7.5 \times 10^4$ T_N/kg based on estimates that quantities exceeding this number would be sufficient to cause GVHD (41). We utilized up to a maximum of 4×10^{10} total nucleated cells including no more than 2×10^{10} $CD45RA^+$ cells from the CD34-depleted fraction for the CD45RA depletion step (the cell numbers were limited by the specifications of the DTS tubing set). The cells were washed and then incubated on a rotator for 30 minutes with one bottle of CD45RA Reagent. After incubation, cells were washed once and then loaded onto the CliniMACS Cell Selection instrument. A DTS tubing set and the Depletion 3.1 program was used for the selection, and the CD45RA-depleted cell population was evaluated for sterility, total nucleated cell count, content of $CD34^+$, $CD3^+$ and $CD3^+CD45RA^+CD45RO^-$ cells, and viability.

Multi-parametric flow cytometric analysis of cell products

Phenotypic characterization of the initial G-PBSC and CD45RA-depleted G-PBSC cell products was performed using a custom LSR II flow cytometer equipped with 405 nm, 488 nm, 532 nm and 635 nm lasers (BD Biosciences). Fluorochrome conjugated mAbs to the following molecules were obtained from BD Biosciences: CD3, CD8, CD4, CD45RO, CD45RA, CD27, CD28, CD19, CD56, CD16, CD14, CD34, IL2 and IFN-γ; antibodies to CD25 and FoxP3 were from eBioscience (San Diego, CA), CCR7 from R & D Systems (Minneapolis, MN), and CD28 from Beckman Coulter (Indianapolis, IN). MHC-tetramer analysis for viral-specific T cells was performed using iTag MHC tetramers purchased from Beckman Coulter. G-PBSC were surface labeled with antibodies or tetramers for 20 or 30 minutes respectively at 4°C. For T regulatory cell analysis, samples were fixed in Fixation Permeabilization solution before washing and staining with anti-FoxP3 mAb in 1X Permeabilization buffer (e-Bioscience). Dead-cell exclusion was performed using either propidium iodide/RNAse staining buffer (BD Biosciences), DAPI (4'6-diamidino-2 phenylindole, Sigma-Aldrich Saint Louis, MO) or Live/Dead Fixable Violet (Molecular Probes, Eugene, OR). Analysis was performed using FlowJo software (Treestar, Ashland, OR).

ELISpot Assays

Libraries of 15-mer overlapping peptides for the following antigens were used in ELISpot assays: CMV (pp65 and IE-1), EBV (BZLF1, EBNA1, and LMP2A) and adenovirus (AdV5 Hexon) (Miltenyi Biotec 'PepTivators'). Prior to performing ELISpot assays to detect antigen-specific T cells, we stimulated aliquots of G-PBSC and CD45RA-depleted G-PBSC once with peptide-pulsed autologous monocyte-derived dendritic cells (moDC) generated according to a modified fast moDC protocol (42). This approach improved the feasibility and reliability of the assays in comparison to a direct ELISpot of the products by circumventing the inhibitory cytokine-mediated suppressive effects of GCSF-exposed monocytes present in G-PBSC on IFNγ release by T cells, and by expanding antigen-specific T cells (43, 44). The ELISpots were performed as described previously (45). Briefly, nitrocellulose-bottomed 96-well plates (MultiScreen MAIP N45, Millipore, Bedford, MA) were coated with an anti-IFN-γ mAb (clone 1-D1K, Mabtech, Stockholm,

Sweden), and nonspecific binding was blocked using 0.5% bovine serum albumin in RPMI 1640. T cells and peptide-pulsed autologous moDC were added to the wells and incubated for 18 hours at 37°C. T cells stimulated with phytohemagglutinin-pulsed moDC (PHA 10 μg/ml Sigma-Aldrich) served as the positive control and T cells exposed to NYBR1 peptide 904 (SLSKILDTV, Genscript) served as the negative control. After washing, biotinylated IFN-γ mAb (clone 7-B6-1, Mabtech), the conjugate (avidin-peroxidase complex; Vectastain avidin-biotin complex method Elite kit; Vector Laboratories, Burlingame, CA), and substrate (Vectastain 3-amino-9-ethylcarbazole substrate) were added according to the manufacturer's instructions. Spot-forming cells were counted by using the Bioreader 5000 optical reader (Bio-sys GMBH, Karben, Germany).

Intracellular cytokine staining

Antigen-specific T cells expanded as described above from G-PBSC or CD45RA-depleted G-PBSC were re-stimulated for 4 hours at 37°C with peptide-pulsed autologous moDC, unpulsed control autologous moDC or autologous lymphoblastoid cell lines in the presence of CD28 and CD49a co-stimulatory mAbs (5μl/ml) (BD Biosciences). Brefeldin A (1 μl/ml Goligplug, BD Biosciences) was added 1.5 hours into the stimulation. The cells were then fixed and permeabilized (Cytofix/Cytoperm, BD Biosciences) and stained with IFN-γ, IL2, CD4 and CD8 fluorescent conjugated mAb (BD Biosciences) in perm wash buffer (BD Biosciences) prior to washing, and data collection on a flow cytometer.

Lymphoproliferation assays

$CD4^+$ T cells were enriched from unmanipulated G-PBSC and CD45RA-depleted G-PBSC by immunomagnetic depletion of other cell subsets ($CD4^+$ T cell isolation kit, Miltenyi Biotec), and plated at 25,000 cells per well in replicate wells (≥4 replicates) of 96 well plates with viral antigen preparations (Microbix Biosystems, Ontario, Canada including 25 μg/ml of cytomegalovirus (CMV, Ad-169), adenovirus (AdV), herpes simplex virus 1 (HSV), varicella zoster (VZV), influenza A (Flu A) and dengue virus (negative control) or PHA (10 μg/ml Sigma-Aldrich, positive control), and irradiated PBSC (2,500 cells/well) to provide antigen presenting cells. The cells were cultured for 6 days with antigen or controls and then pulsed with 1 μCi of ^3H thymidine during the final 20 hours of the assay before harvesting and scintillation counting (Perkin Elmer, Waltham, MA).

Statistical analysis

Statistical analysis was conducted using Prism Software (GraphPad). Student's t test was conducted as a two-tailed paired test with a confidence interval of 95% and results with a P value of <0.05 were considered significant.

Results

Design of a cell selection strategy using anti CD45RA to deplete T_N cells from G-PBSC

Human T_N uniformly express the high molecular weight CD45RA isoform of the hematopoietic cell-specific tyrosine phosphatase CD45, and express several other cell surface markers including CD62L, CCR7, CD27 and CD28 (22–25, 27). We considered using anti-CD62L mAb to deplete T_N consistent with the approach taken in the original

murine studies that demonstrated that donor T_N were the most potent subset for causing GVHD (28). However, CD62L is subject to proteolytic cleavage by ADAM-17 and other metalloproteases released during G-CSF mobilization of PBSC (46), and we found that cell surface CD62L expression substantially declined on T cells in G-PBSC products stored over 24 hours (Figure 1A). Moreover, CD62L is also expressed on T_{CM} and using this marker for depletion would remove a potentially critical subset for robust immune reconstitution (24, 47, 48). In contrast, CD45RA was not subject to proteolytic cleavage in G-PBSC (Figure 1A) and is absent on most memory T cells, including T_{CM}. The $CD45RA^+$ 'T_{EMRA}' subset of T_M, will be removed by CD45RA depletion, but it would be anticipated that donor T_{CM} transferred in the CD45RA-depleted PBSC will repopulate the T_{EMRA} subset based on recent studies demonstrating that T cell differentiation follows a linear pathway in which T_{CM} giving rise to T_{EM} and to effector T cell subsets (48, 49).

Further analysis of CD45RA as a target to deplete T_N from G-PBSC revealed some limitations. First, polymorphisms in the *CD45* gene have been described (50), and one variant (allele frequency 0–3.5%) is a C77G point mutation in a splice silencer region in exon 4 that prevents excision of the exon, resulting in retention of CD45RA expression on memory T cells. To estimate the frequency of aberrant *CD45* expression in our community, we first evaluated expression of CD45RA and CD45RO on T cells in 50 normal donors by flow cytometry and identified a phenotype consistent with the C77G variant in two donors (4%) (Figure 1B). This result indicated it would be desirable to screen HCT donors for this variant and exclude this minor subset of donors from future clinical trials, since $CD45RA^+$ depletion would remove all T cells from PBSC products from such individuals. Second, there are reports that a minor subset of $CD34^+$ stem cells expresses CD45RA, and that the $CD45RA^+CD34^+$ subset is enriched for granulocyte macrophage and megakaryocyte colony forming units relative to $CD45RA^-CD34^+$ cells (51). Staining aliquots of G-PBSC with both mAb confirmed that a significant subset of $CD34^+$ cells co-expressed CD45RA (Figure 1C). Thus, to preserve all subsets of $CD34^+$ stem cells in the graft, it was necessary to develop a two-step immunomagnetic selection procedure involving a positive selection of $CD34^+$ progenitor cells using anti-CD34mAb conjugated beads followed by depletion of $CD45RA^+$ cells from the CD34-negative fraction (Figure 2).

Evaluation of sequential positive and negative selection for preparing G-PBSC depleted of naïve T cells

We processed G-PBSC from fifteen consecutive normal stem cell donors using the two-step selection method. For ten donors, sufficient $CD34^+$ cells were obtained from a single apheresis collection to proceed directly with cell selection, and for five donors the cell selections were performed after pooling two apheresis samples collected on consecutive days. The CD34 selection provided products with a median purity of 97.6% (range 92.5–98.7%) $CD34^+$ cells, a yield of 73% (range 60–81%), and a residual median $CD3^+$ T cell content of 0.26% (range 0.09–1.3%). These purities and yields are comparable to the values previously reported for $CD34^+$ selection using the CliniMACS CD34 reagent system (39).

CD45RA depletion was then performed on the CD34-depleted product and consistently resulted in near complete depletion of $CD45RA^+$ T cells (Figure 3A and 3B). An aliquot of

cells from the CD45RA-depleted products of each of the 15 donors could be removed (representing a median of 26% of the available cells; range 10–65%) to achieve our target doses of 1×10^7 $CD3^+$ cells/kg and $<7.5 \times 10^4$ T_N cells/kg. The median residual T_N cell content of the CD45RA-depleted aliquot that contained 1×10^7 T_M/kg was 0.12×10^4/kg (range $0.02–0.65 \times 10^4$/kg). The fifteen donor G-PBSC products that were processed by sequential CD34-selection and CD45RA-depletion were composed of a median of 8.47×10^6/kg $CD34^+$ cells/kg (range 5.29-14.33 $CD34^+$/kg), 0.36×10^4 T_N/kg (range $0.09–0.78 \times 10^4$ T_N/kg) and 9.99×10^6 T_M/kg (range $9.94–10.03 \times 10^6$ T_M/kg) (Figures 3C and 3D). The residual T_N cells in the cell product were approximately evenly distributed between the $CD34^+$ cell component and the CD45RA-depleted component (Figure 3E). The viability of the cell products was consistently high at the end of cell processing for both the $CD34^+$-enriched and CD45RA-depleted components ($CD34^+$ median 98.4%, range 96.2–99.3%; CD45RA-depleted median 97.7%, range 96.3–98.8%), and all products met sterility release criteria.

Cellular composition of CD45RA-depleted G-PBSC

The two-step cell selection was highly effective in removing $CD3^+CD45RA^+CD45RO^-$ T_N from G-PBSC. However CD45RA is expressed on other hematopoietic cells, including most B-cells, NK cells, and a subpopulation of Tregs (52). We therefore analyzed the cell composition of G-PBSCs prior to cell selection, and of an aliquot of CD45RA-depleted G-PBSC prepared for infusion. In addition to the profound reduction ($4.5 – 5$ $\log_{10}$) in T_N cells, we observed a $4.5 – 5.0$ $\log_{10}$ reduction in $CD45RA^+$ Tregs ($CD45RA^+CD4^+CD3^+CD25^+FOXP3^+$) and total B cells and a 3.4 $\log_{10}$ reduction in total NK cells (Table 1). Also observed was a 1–2 $\log_{10}$ reduction in total nucleated cells (TNC), monocytes, total $CD3^+$ T cells, $CD4^+CD3^+$ and $CD8^+CD3^+$ T cells, and $CD4^+CD3^+$ $CD25^+$ $FOXP3^+$ Tregs compared to the composition of the unselected product, partially as a consequence of limiting the T cell content to 1×10^7 TM cells/kg in the selected product. There was minimal variation in the composition of the 15 cell products after the selection procedure (Figure 4). The T_M cells in the CD45RA-depleted product were comprised of approximately 80% $CD4^+$ (range 65–93%) and 20% $CD8^+$ T cells (range 6–32%). The frequency of $CD8^+$ T cells in the CD45RA-depleted product that expressed a $CD3^+CD8^+CD45RO^+CD45RA^-CCR7^+CD27^+CD28^+$ T_{CM} phenotype was 32.7% (range 21.3–68.7%) compared to 4.03% (range 1–14.3%) in unmanipulated G-PBSCs. The frequency of $CD4^+$ T cells in the final product that expressed a $CD3^+CD4^+CD45RO^+CD45RA^-CCR7^+CD27^+CD28^+$ T_{CM} phenotype was 68.4% (49.5–84.2%) compared to 20.5% (9.3–39.4%) in the unmanipulated G-PBSC.

Functional pathogen-specific T cells are retained in CD45RA-depleted G-PBSC

A theoretical advantage of CD45RA-depleted PBSC over complete TCD as a strategy for HCT is that pathogen-specific T_M cells should be retained in the graft and could transfer protective immunity to opportunistic infections such as CMV and EBV. We used MHC tetramer analysis to enumerate T cells specific for immunodominant epitopes from CMV (pp65, NLVPMVATV) and EBV (BMLF1, GLCTLVAML) in G-PBSC and CD45RA-depleted PBSC from a subset of donors who expressed the HLA-A*0201 restricting allele and were seropositive for CMV and EBV. EBV GLC-specific T cells were present in a

similar proportion of the $CD8^+$ T cell population in PBSC and CD45RA-depleted PBSC. Although CMV NLV-specific T cells were observed in lower frequencies in the CD45RA-depleted PBSC, this population included a higher proportion of virus-specific T cells that expressed CD28 and CCR7 consistent with a T_{CM} phenotype, implying an enhanced capacity to persist and expand *in vivo* (Figure 5). T cells specific for most other viral antigens are present at low levels in peripheral blood and PBSC, and direct analysis is not feasible. Moreover, direct functional analysis of antigen-specific T cells in G-PBSC is impaired because of the cytokine-mediated suppressive effects of GCSF-exposed monocytes (43, 44). To overcome these obstacles, we measured opportunistic virus-specific T cell responses in G-PBSC and CD45RA-depleted G-PBSC after short-term *in vitro* T cell expansion. Aliquots of G-PBSC and CD45RA-depleted G-PBSC were stimulated with autologous moDC pulsed with pools of 15 mer peptides spanning the products of genes that are known to encode immunodominant epitopes from CMV (pp65 and IE-1), EBV (BZLF1, EBNA1, and LMP2A) and adenovirus (AdV5 Hexon), and then assayed on day ten after stimulation by interferon gamma (IFNγ) ELISpot. T cell responses to CMV (CMVpp65 and or IE-1) were observed in both the CD45RA-depleted and unmanipulated G-PBSC obtained from each of the five CMV positive donors, but not the two CMV seronegative donors, confirming that the assay detected memory T cell responses. T cells that produced IFNγ specifically in response to restimulation with adenovirus and EBV antigens (BZLF, EBNA1, or LMP2A) were also present the CD45RA-depleted G-PBSC whenever they were detected in unmanipulated G-PBSC (Figure 6 A-C), confirming retention of memory T cells to a range of pathogens after CD45RA depletion.

The ELISpot assays only measured IFNγ production and did not distinguish responses of $CD4^+$ and $CD8^+$ T cell subsets. The recovery of multifunctional $CD4^+$ and $CD8^+$ virus-specific T cells, defined as those capable of producing both IFNγ and IL2, has been associated with superior protection in HCT recipients (53, 54). Therefore, we evaluated IFNγ and IL2 secretion by virus-specific $CD4^+$ and $CD8^+$ T cells expanded from G-PBSC and from CD45RA-depleted G-PBSC using 15 mer peptide pools for EBNA-1 and pp65. We detected an equivalent or higher frequency of multifunctional virus-specific $CD4^+$ and $CD8^+$ T cells in CD45RA-depleted products, consistent with the removal of $CD45RA^+$ naïve T cells that would be unresponsive in the assay and elimination of the subset of $CD45RA^+$ effector memory T cells that are less commonly multifunctional (Figure 7A-C) (55).

Whole protein antigens that are processed through the MHC class II antigen processing pathway for presentation to $CD4^+$ T cells are available for more pathogens, and encompass a larger number of potential epitopes than peptide pools. We used protein antigen preparations for several viruses that can cause serious infection in HCT recipients, specifically CMV, AdV, herpes simplex virus (HSV), varicella zoster virus (VZV), and influenza A (Flu A) in lymphoproliferative assays to evaluate the retention of virus-specific $CD4^+$ T cells in CD45RA-depleted PBSC. In these experiments, $CD4^+$ T cells were first enriched from unmanipulated G-PBSC and CD45RA-depleted G-PBSC by immunomagnetic depletion of other hematopoietic cell subsets and plated in 96 well plates with media alone, dengue virus antigen preparation (negative control), PHA (positive control), or with each of the HCT

virus antigen preparations. All four CMV-seropositive donors but not the two CMV-seronegative donor showed a significant $CD4^+$ proliferative response to CMV antigen in both the unmanipulated G-PBSC and CD45RA-depleted G-PBSC. Strong specific $CD4^+$ proliferative responses were also observed against AdV, HSV, VZV and Flu A in the unmanipulated G-PBSC and CD45RA-depleted G-PBSC (Figure 8). Thus, preparing a G-PBSC product that is depleted of $CD45RA^+$ T_N and contains a fixed dose of 1×10^7 T_M cells/kg preserves multifunctional $CD4^+$ and $CD8^+$ T cells capable of specifically responding to viral antigens.

Discussion

Evidence from animal models demonstrates that the diverse T_N subset has the greatest potential to cause GVHD after allogeneic HCT (28–37). Prior studies in our lab have also shown that purified $CD8^+$ T_N from HLA-identical sibling donors mediate markedly greater reactivity for disparate minor H antigens in limiting dilution cultures than purified $CD8^+$ T_M suggesting that the *in vivo* murine model data may apply to humans (38). As a prelude to translating the insights derived from the murine model to the clinic, we developed a novel, two-step, clinically compliant procedure for manipulating G-PBSC to remove T_N, preserve $CD34^+$ hematopoietic stem cells, and provide for a fixed dose of T_M cells that includes T cells with specificity for common opportunistic pathogens encountered after HCT. Our studies of fifteen consecutive G-GSCF mobilized PBSC products demonstrate reproducible performance of an immunomagnetic cell selection procedure that first positively selects $CD34^+$ cells and then depletes $CD45RA^+$ T_N from the CD34 negative fraction. The rationale for first positively selecting $CD34^+$ cells was based on our desire to preserve the subset of $CD34^+$ cells that express CD45RA and prior data demonstrating that purified $CD34^+$ cells selected on the Miltenyi CliniMACS have high engraftment potential (20, 51, 56). Consistent with previous experience, the positive selection of $CD34^+$ progenitor cells resulted in a cell product of high purity, reasonable yield and a very low residual T cell content (39). In the second-step, $CD45RA^+$ T_N were effectively depleted from the CD34-depleted fraction using a newly developed clinical grade αCD45RA immunomagnetic bead. Both $CD34^+$ and CD45RA-depleted products retained high viability during cell processing, and the resulting cell products consistently met the target cell doses of $>5 \times 10^6$ $CD34^+$ cells/kg, 1×10^7 T_M /kg and $<7.5\times 10^4$ T_N /kg. This efficient and reliable method for depleting T_N enables clinical evaluation of the outcome of HLA-matched allogeneic HCT using donor PBSC grafts that contain $CD34^+$ stem cells, a fixed number of T_M cells, and minimal contaminating T_N cells.

A major conceptual advantage of PBSC transplants selectively depleted of T_N compared with complete TCD is the potential to retain functional donor T_M specific for opportunistic pathogens that can confer protection against infection. Our data show that both $CD4^+$ and $CD8^+$ T_M cells are contained within the CD45RA-depleted G-PBSC product, and each of these subsets are enriched for cells with a T_{CM} phenotype. T_{CM} cells have high replicative potential and can both self-renew and differentiate to T_{EM} and T_E cell subsets *in vivo* (21, 24, 47, 48). The CD34 selection and CD45RA-depletion procedures do not interfere with function of the remaining T_M cells. Our data demonstrate that after cell processing, the T_M cells are capable of proliferating and producing effector cytokines in response to common

opportunistic viruses including CMV, EBV, AdV, HSV and VZV. Consistent with the preponderance of T cells with a T_{CM} phenotype, multifunctional $CD4^+$ and $CD8^+$ T cells that secreted IL2 and IFNγ in response to viral antigen were prevalent in the CD45RA-depleted G-PBSC. Thus, it is predicted that recovery of T cell numbers and pathogen-specific immunity would be improved in the early post HCT period with a CD45RA-depleted graft compared to a graft completely depleted of T cells (24, 47).

A disadvantage of the T_N depletion approach is that it would not remove donor T_M that were elicited by prior exposure through pregnancy or blood transfusion to minor H antigens that may be shared by the transplant recipient, or that are pathogen-specific but cross-reactive with an alloantigen expressed by the recipient. Some studies in murine models of GVHD have shown that T_{CM} can contribute to GVHD although the severity and lethality of GVHD is consistently higher in mice that receive T_N than either T_M subset (34, 37). Whether the GVHD in these models represents cross-reactivity, or differences in the composition of the T_{CM} pool in young laboratory mice with limited pathogen exposure is uncertain. Limiting dilution assays have demonstrated that cross-reactive recognition of minor H antigens by human T_M is extremely infrequent (38). Recognition of disparate MHC molecules by T_M is more frequent (57–59), suggesting this approach may have less merit in the MHC-mismatched allogeneic HCT setting than alternative approaches that specifically remove T cells activated by allogeneic stimulation. Thus, the logical clinical setting to first test T_N depletion would be in HLA-identical allogeneic HCT where the donor is nonparous and has not had prior blood transfusions, and a clinical trial of this approach is in progress at our institutions.

The complexity of cell processing for CD45RA-depletion is substantially less than alternative forms of selective-depletion of alloreactive T cells that are being investigated in other clinical trials such as *in vitro* stimulation of T cells in PBSC products followed 2–5 days later by depletion of activated alloreactive T cells using immunomagnetic beads, immunotoxins, fluorescent activated cell sorting, or photodynamic purging (60). The cell selection procedure we describe is viewed by the FDA as involving “minimal manipulation”, can be completed in eight hours in a clinical hematopoietic stem cell processing laboratory, and does not require GMP conditions. Therefore, if CD45RA-depletion proves to be successful in reducing GVHD and providing adequate immune reconstitution in clinical trials, the wider HCT community could readily adopt this technology. The cost of the two-stage cell selection procedure including reagents and labor is less than $20,000. Although the upfront cost is substantial, if CD45RA-depletion is effective in preventing serious or chronic GVHD and opportunistic infections, it is likely to be cost effective when one considers the cost of post-HCT care for GVHD (procedures, medications, hospitalizations) and severe opportunistic infections (medications, hospitalization, ICU costs). Furthermore, the cost of CD45RA-depletion compares favorably to alternative new forms of *in vitro* T cell depletion such as the depletion of $\alpha\beta$ T cells and B cells from PBSC.

Acknowledgments

The authors would like to thank Su Yi, Andrew Mackie, Julia Richardt, Sarah Click and Tanya Budiarto for expert technical assistance. This work was supported by grants NIH CA18029, CA 136551, CA15704, and DK56465 and by the NIH Rapid Access to Intervention Development (RAID, project 298). Warren Shlomchik is the recipient of support from the Burroughs Wellcome Fund and was a Leukemia and Lymphoma Society Clinical Scholar. Marie Bleakley is the Damon Runyon-Richard Lumsden Foundation Clinical Investigator supported in part by the Damon Runyon Cancer Research Foundation (CI-57-11), and received support from K23CA154532 from the National Cancer Institute and previously from a Special Fellowship in Clinical Research from the Leukemia and Lymphoma Society.

References

1. Ferrara JL, Levine JE, Reddy P, Holler E. Graft-versus-host disease. Lancet. 2009; 373:1550–1561. [PubMed: 19282026]
2. Chao NJ. Minors come of age: Minor histocompatibility antigens and graftversus- host disease. Biol Blood Marrow Transplant. 2004; 10:215–223. [PubMed: 15077220]
3. Ferrara JL, Reddy P. Pathophysiology of graft-versus-host disease. Semin Hematol. 2006; 43:3–10. [PubMed: 16412784]
4. Shlomchik WD. Graft-versus-host disease. Nat Rev Immunol. 2007; 7:340–352. [PubMed: 17438575]
5. Bensinger WI, Martin PJ, Storer B, et al. Transplantation of bone marrow as compared with peripheral-blood cells from HLA-identical relatives in patients with hematologic cancers. N Engl J Med. 2001; 344:175–181. [PubMed: 11172139]
6. Mielcarek M, Storer B, Martin PJ, et al. Long-term outcomes after transplantation of HLA-identical related G-CSF-mobilized peripheral blood mononuclear cells versus bone marrow. Blood. 2012; 119:2675–2678. [PubMed: 22308289]
7. Oehler VG, Radich JP, Storer B, et al. Randomized trial of allogeneic related bone marrow transplantation versus peripheral blood stem cell transplantation for chronic myeloid leukemia. Biol Blood Marrow Transplant. 2005; 11:85–92. [PubMed: 15682068]
8. Ratanatharathorn V, Nash RA, Przepiorka D, et al. Phase III study comparing methotrexate and tacrolimus (prograf, FK506) with methotrexate and cyclosporine for graft-versus-host disease prophylaxis after HLA-identical sibling bone marrow transplantation. Blood. 1998; 92:2303–2314. [PubMed: 9746768]
9. Korngold R, Sprent J. Lethal graft-versus-host disease after bone marrow transplantation across minor histocompatibility barriers in mice. Prevention by removing mature T cells from marrow. J Exp Med. 1978; 148:1687–1698. [PubMed: 363972]
10. Martin PJ, Hansen JA, Buckner CD, et al. Effects of in vitro depletion of T cells in HLA-identical allogeneic marrow grafts. Blood. 1985; 66:664–672. [PubMed: 3896348]
11. Keever CA, Small TN, Flomenberg N, et al. Immune reconstitution following bone marrow transplantation: comparison of recipients of T-cell depleted marrow with recipients of conventional marrow grafts. Blood. 1989; 73:1340–1350. [PubMed: 2649174]
12. Small TN, Papadopoulos EB, Boulad F, et al. Comparison of immune reconstitution after unrelated and related T-cell-depleted bone marrow transplantation: effect of patient age and donor leukocyte infusions. Blood. 1999; 93:467–480. [PubMed: 9885208]
13. Champlin RE, Passweg JR, Zhang MJ, et al. T-cell depletion of bone marrow transplants for leukemia from donors other than HLA-identical siblings: advantage of T-cell antibodies with narrow specificities. Blood. 2000; 95:3996–4003. [PubMed: 10845940]
14. Ho VT, Soiffer RJ. The history and future of T-cell depletion as graft-versus-host disease prophylaxis for allogeneic hematopoietic stem cell transplantation. Blood. 2001; 98:3192–3204. [PubMed: 11719354]
15. Barker JN, Hough RE, van Burik JA, et al. Serious infections after unrelated donor transplantation in 136 children: impact of stem cell source. Biol Blood Marrow Transplant. 2005; 11:362–370. [PubMed: 15846290]

16. Jakubowski AA, Small TN, Young JW, et al. T cell depleted stem-cell transplantation for adults with hematologic malignancies: sustained engraftment of HLA-matched related donor grafts without the use of antithymocyte globulin. Blood. 2007; 110:4552–4559. [PubMed: 17717135]
17. Almyroudis NG, Jakubowski A, Jaffe D, et al. Predictors for persistent cytomegalovirus reactivation after T-cell-depleted allogeneic hematopoietic stem cell transplantation. Transpl Infect Dis. 2007; 9:286–294. [PubMed: 17511819]
18. van Burik JA, Carter SL, Freifeld AG, et al. Higher risk of cytomegalovirus and aspergillus infections in recipients of T cell-depleted unrelated bone marrow: analysis of infectious complications in patients treated with T cell depletion versus immunosuppressive therapy to prevent graft-versus-host disease. Biol Blood Marrow Transplant. 2007; 13:1487–1498. [PubMed: 18022579]
19. Keever-Taylor CA, Wagner JE, Kernan NA, et al. Comparison of immune recovery in recipients of unmanipulated vs T-cell-depleted grafts from unrelated donors in a multicenter randomized phase II-III trial (T-cell depletion trial). Bone Marrow Transplant. 2010; 45:587–589. [PubMed: 19617904]
20. Devine SM, Carter S, Soiffer RJ, et al. Low risk of chronic graft-versus-host disease and relapse associated with T cell-depleted peripheral blood stem cell transplantation for acute myelogenous leukemia in first remission: results of the blood and marrow transplant clinical trials network protocol 0303. Biol Blood Marrow Transplant. 2011; 17:1343–1351. [PubMed: 21320619]
21. Sallusto F, Lenig D, Forster R, Lipp M, Lanzavecchia A. Two subsets of memory T lymphocytes with distinct homing potentials and effector functions. Nature. 1999; 401:708–712. [PubMed: 10537110]
22. Lanzavecchia A, Sallusto F. Dynamics of T lymphocyte responses: intermediates, effectors, and memory cells. Science. 2000; 290:92–97. [PubMed: 11021806]
23. Kaech SM, Ahmed R. Memory CD8+ T cell differentiation: initial antigen encounter triggers a developmental program in naive cells. Nat Immunol. 2001; 2:415–422. [PubMed: 11323695]
24. Wherry EJ, Teichgraber V, Becker TC, et al. Lineage relationship and protective immunity of memory CD8 T cell subsets. Nat Immunol. 2003; 4:225–234. [PubMed: 12563257]
25. Sallusto F, Geginat J, Lanzavecchia A. Central memory and effector memory T cell subsets: function, generation, and maintenance. Annu Rev Immunol. 2004; 22:745–763. [PubMed: 15032595]
26. Willinger T, Freeman T, Hasegawa H, McMichael AJ, Callan MF. Molecular signatures distinguish human central memory from effector memory CD8 T cell subsets. J Immunol. 2005; 175:5895–5903. [PubMed: 16237082]
27. Ahmed R, Bevan MJ, Reiner SL, Fearon DT. The precursors of memory: models and controversies. Nat Rev Immunol. 2009; 9:662–668. [PubMed: 19680250]
28. Anderson BE, McNiff J, Yan J, et al. Memory CD4+ T cells do not induce graftversus- host disease. J Clin Invest. 2003; 112:101–108. [PubMed: 12840064]
29. Sondel PM, Buhtoiarov IN, DeSantes K. Pleasant memories: remembering immune protection while forgetting about graft-versus-host disease. J Clin Invest. 2003; 112:25–27. [PubMed: 12840055]
30. Zhang Y, Joe G, Zhu J, et al. Dendritic cell-activated CD44hiCD8+ T cells are defective in mediating acute graft-versus-host disease but retain graft-versus-leukemia activity. Blood. 2004; 103:3970–3978. [PubMed: 14764532]
31. Chen BJ, Cui X, Sempowski GD, Liu C, Chao NJ. Transfer of allogeneic CD62Lmemory T cells without graft-versus-host disease. Blood. 2004; 103:1534–1541. [PubMed: 14551132]
32. Xystrakis E, Bernard I, Dejean AS, Alsaati T, Druet P, Saoudi A. Alloreactive CD4 T lymphocytes responsible for acute and chronic graft-versus-host disease are contained within the CD45RChigh but not the CD45RClow subset. Eur J Immunol. 2004; 34:408–417. [PubMed: 14768045]
33. Dutt S, Tseng D, Ermann J, et al. Naive and memory T cells induce different types of graft-versus-host disease. J Immunol. 2007; 179:6547–6554. [PubMed: 17982043]
34. Chen BJ, Deoliveira D, Cui X, et al. Inability of memory T cells to induce graftversus- host disease is a result of an abortive alloresponse. Blood. 2007; 109:3115–3123. [PubMed: 17148592]

35. Zheng H, Matte-Martone C, Li H, et al. Effector memory CD4+ T cells mediate graft-versus-leukemia without inducing graft-versus-host disease. Blood. 2008; 111:2476–2484. [PubMed: 18045967]
36. Anderson BE, Zheng H, Taylor PA, et al. Memory T cells in GVHD and GVL. Biol Blood Marrow Transplant. 2008; 14:19–20. [PubMed: 19418622]
37. Zheng H, Matte-Martone C, Jain D, McNiff J, Shlomchik WD. Central memory CD8+ T cells induce graft-versus-host disease and mediate graft-versus-leukemia. J Immunol. 2009; 182:5938–5948. [PubMed: 19414745]
38. Bleakley M, Otterud BE, Richardt JL, et al. Leukemia-associated minor histocompatibility antigen discovery using T-cell clones isolated by in vitro stimulation of naive CD8+ T cells. Blood. 2010; 115:4923–4933. [PubMed: 20203263]
39. Keever-Taylor CA, Devine SM, Soiffer RJ, et al. Characteristics of CliniMACS(R) System CD34-enriched T cell-depleted grafts in a multicenter trial for acute myeloid leukemia-Blood and Marrow Transplant Clinical Trials Network (BMT CTN) protocol 0303. Biol Blood Marrow Transplant. 2012; 18:690–697. [PubMed: 21875505]
40. Collins NH, Gee AP, Durett AG, et al. The effect of the composition of unrelated donor bone marrow and peripheral blood progenitor cell grafts on transplantation outcomes. Biol Blood Marrow Transplant. 2010; 16:253–262. [PubMed: 19822219]
41. Kernan NA, Collins NH, Juliano L, Cartagena T, Dupont B, O'Reilly RJ. Clonable T lymphocytes in T cell-depleted bone marrow transplants correlate with development of graft-v-host disease. Blood. 1986; 68:770–773. [PubMed: 3527302]
42. Dauer M, Obermaier B, Herten J, et al. Mature dendritic cells derived from human monocytes within 48 hours: a novel strategy for dendritic cell differentiation from blood precursors. J Immunol. 2003; 170:4069–4076. [PubMed: 12682236]
43. Boneberg EM, Hareng L, Gantner F, Wendel A, Hartung T. Human monocytes express functional receptors for granulocyte colony-stimulating factor that mediate suppression of monokines and interferon-gamma. Blood. 2000; 95:270–276. [PubMed: 10607712]
44. Saito M, Kiyokawa N, Taguchi T, et al. Granulocyte colony-stimulating factor directly affects human monocytes and modulates cytokine secretion. Exp Hematol. 2002; 30:1115–1123. [PubMed: 12384141]
45. Scheibenbogen C, Lee KH, Mayer S, et al. A sensitive ELISPOT assay for detection of CD8+ T lymphocytes specific for HLA class I-binding peptide epitopes derived from influenza proteins in the blood of healthy donors and melanoma patients. Clin Cancer Res. 1997; 3:221–226. [PubMed: 9815676]
46. Smalley DM, Ley K. L-selectin: mechanisms and physiological significance of ectodomain cleavage. J Cell Mol Med. 2005; 9:255–266. [PubMed: 15963248]
47. Berger C, Jensen MC, Lansdorp PM, Gough M, Elliott C, Riddell SR. Adoptive transfer of effector CD8+ T cells derived from central memory cells establishes persistent T cell memory in primates. J Clin Invest. 2008; 118:294–305. [PubMed: 18060041]
48. Buchholz VR, Flossdorf M, Hensel I, et al. Disparate Individual Fates Compose Robust CD8+ T Cell Immunity. Science. 2013
49. Buchholz VR, Graf P, Busch DH. The smallest unit: effector and memory CD8(+) T cell differentiation on the single cell level. Front Immunol. 2013; 4:31. [PubMed: 23424063]
50. Tchilian EZ, Beverley PC. Altered CD45 expression and disease. Trends Immunol. 2006; 27:146–153. [PubMed: 16423560]
51. Bender JG, Unverzagt K, Walker DE, et al. Phenotypic analysis and characterization of CD34+ cells from normal human bone marrow, cord blood, peripheral blood, and mobilized peripheral blood from patients undergoing autologous stem cell transplantation. Clin Immunol Immunopathol. 1994; 70:10–18. [PubMed: 7505211]
52. Miyara M, Yoshioka Y, Kitoh A, et al. Functional delineation and differentiation dynamics of human CD4+ T cells expressing the FoxP3 transcription factor. Immunity. 2009; 30:899–911. [PubMed: 19464196]

53. Zhou W, Longmate J, Lacey SF, et al. Impact of donor CMV status on viral infection and reconstitution of multifunction CMV-specific T cells in CMV-positive transplant recipients. Blood. 2009; 113:6465–6476. [PubMed: 19369230]
54. Lilleri D, Fornara C, Chiesa A, Caldera D, Alessandrino EP, Gerna G. Human cytomegalovirus-specific CD4+ and CD8+ T-cell reconstitution in adult allogeneic hematopoietic stem cell transplant recipients and immune control of viral infection. Haematologica. 2008; 93:248–256. [PubMed: 18245650]
55. Faint JM, Annels NE, Curnow SJ, et al. Memory T cells constitute a subset of the human CD8+CD45RA+ pool with distinct phenotypic and migratory characteristics. J Immunol. 2001; 167:212–220. [PubMed: 11418651]
56. Handgretinger R, Klingebiel T, Lang P, et al. Megadose transplantation of purified peripheral blood CD34(+) progenitor cells from HLA-mismatched parental donors in children. Bone Marrow Transplant. 2001; 27:777–783. [PubMed: 11477433]
57. Melenhorst JJ, Scheinberg P, Williams A, et al. Alloreactivity Across HLA Barriers Is Mediated by Both Naive and Antigen-Experienced T Cells. Biol Blood Marrow Transplant. 2011
58. Burrows SR, Khanna R, Burrows JM, Moss DJ. An alloresponse in humans is dominated by cytotoxic T lymphocytes (CTL) cross-reactive with a single Epstein-Barr virus CTL epitope: implications for graft-versus-host disease. J Exp Med. 1994; 179:1155–1161. [PubMed: 7511682]
59. Burrows SR, Khanna R, Silins SL, Moss DJ. The influence of antiviral T-cell responses on the alloreactive repertoire. Immunol Today. 1999; 20:203–207. [PubMed: 10322297]
60. Mielke S, Solomon SR, Barrett AJ. Selective depletion strategies in allogeneic stem cell transplantation. Cytotherapy. 2005; 7:109–115. [PubMed: 16040390]

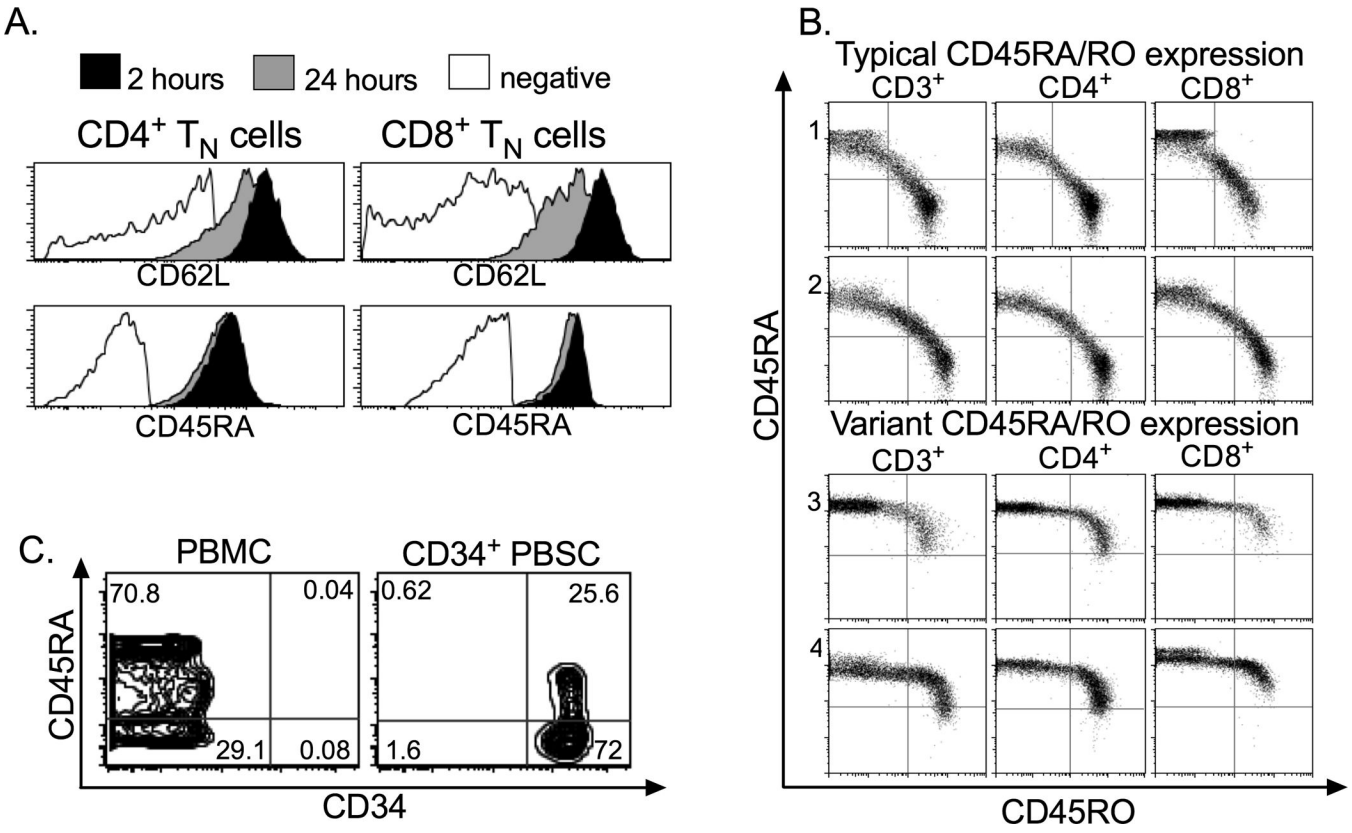

Figure 1. Flow cytometric analysis of normal donor blood cells

Blood cells obtained from normal donors were analyzed by flow cytometry to assist in designing of a cell selection strategy to deplete T_N from G-PBSC. A) Stability of CD62L and CD45RA expression on $CD4^+$ or $CD8^+$ T cells in G-PBSC at 2 and 24 hours after apheresis collection (live $CD3^+$ lymphocyte gate). B) Expression of CD45RA and CD45RO on $CD3^+$, $CD4^+$, and $CD8^+$ T cells in normal donors with the typical (panels 1 and 2) and variant patterns of CD45 expression (panels 3 and 4). Data is shown after gating on live lymphocytes. C) CD45RA is expressed on a minor subset of $CD34^+$ cells in samples of normal donor PBMC, or $CD34^+$ cells isolated by positive immunomagnetic selection from G-PBSC.

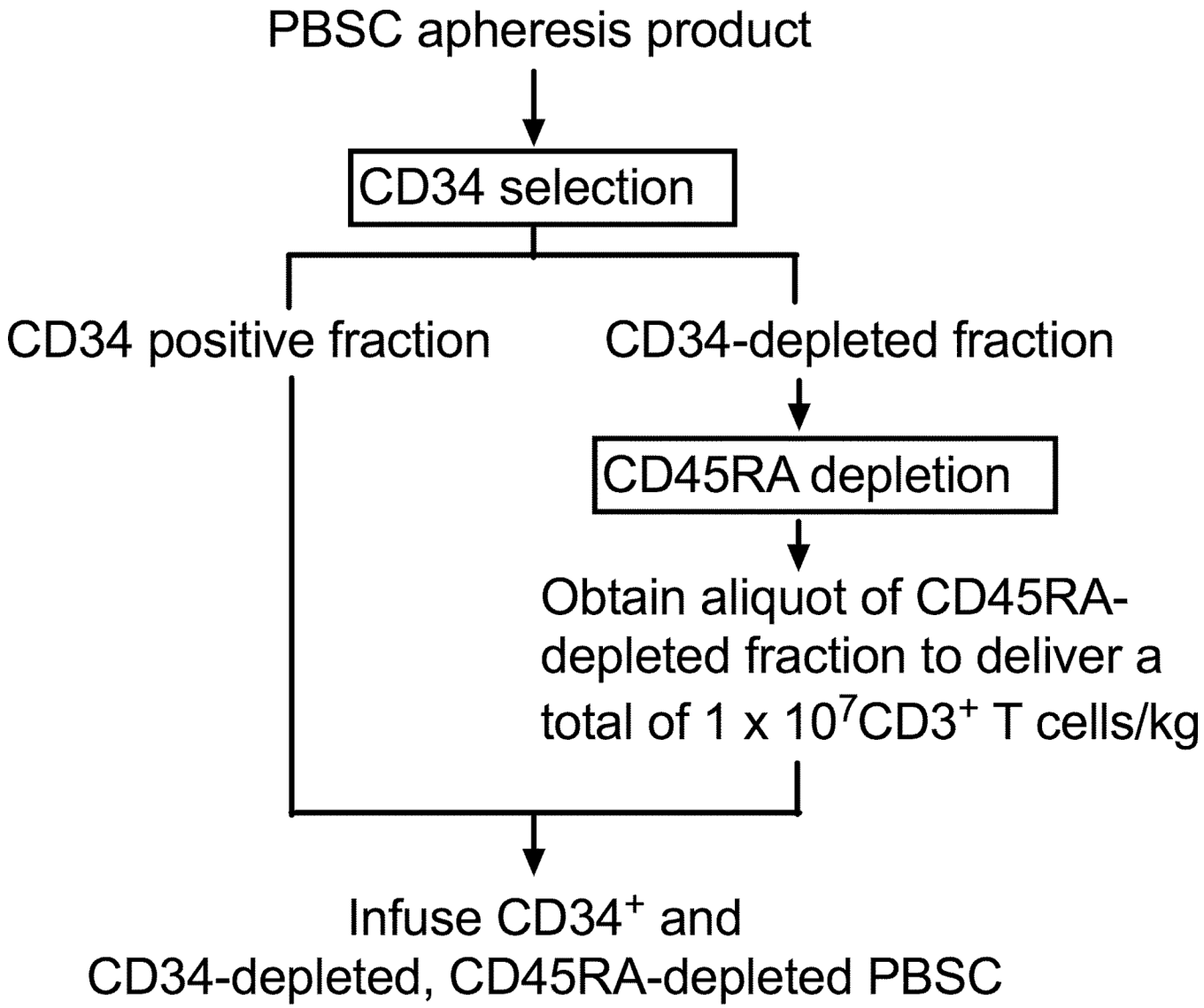

Figure 2. Cell selection procedure

The flow diagram depicts the cell processing procedure to deplete T_N from G-PBSC, preserve $CD34^+$ stem cells and deliver a fixed dose of T_M cells.

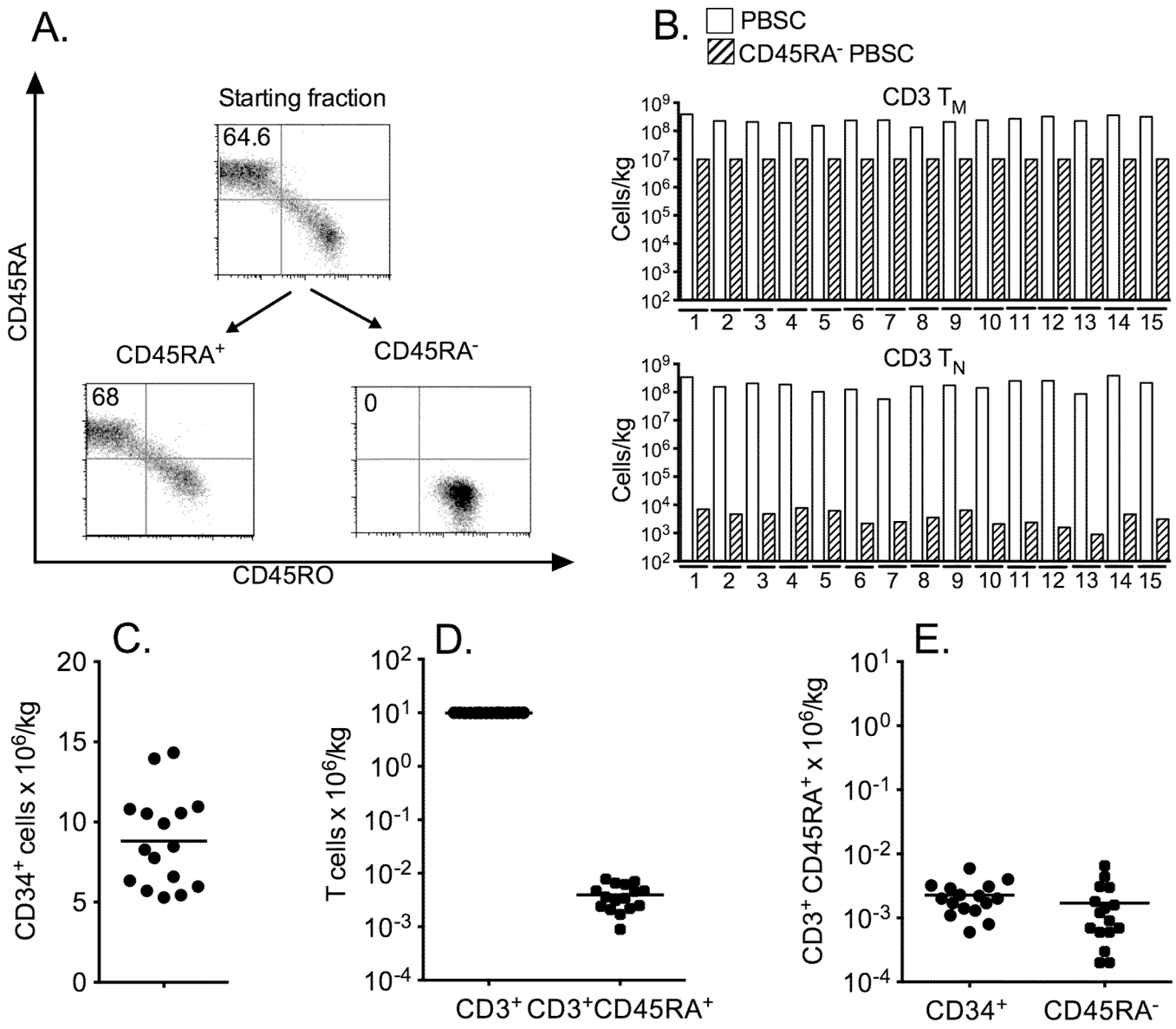

Figure 3. Results of cell selection procedures

A) T_N ($CD45RA^+CD45RO^-CD3^+$) content of (CD34-depleted) G-PBSC product, CD45RA-depleted fraction, and $CD45RA^+$ fraction from cell selection on G-PBSC from a representative donor (gated on live $CD3^+$ T cells). B) $CD3^+$ T_N content in the initial G-PBSC and in an aliquot prepared for infusion after depletion of $CD45RA^+$ cells on 15 representative donors after adjusting the $CD3^+$ T_M content in the $CD45RA^-$ fraction to 10^7 cells/kg. C) Total $CD34^+$ cell content and D) $CD3^+$ and T_N $CD3^+CD45RA^+$ content of the infused cell products. E) T_N ($CD3^+CD45RA^+$) content in the $CD34^+$ fraction and in the $CD34^-$, CD45RA-depleted cell fraction.

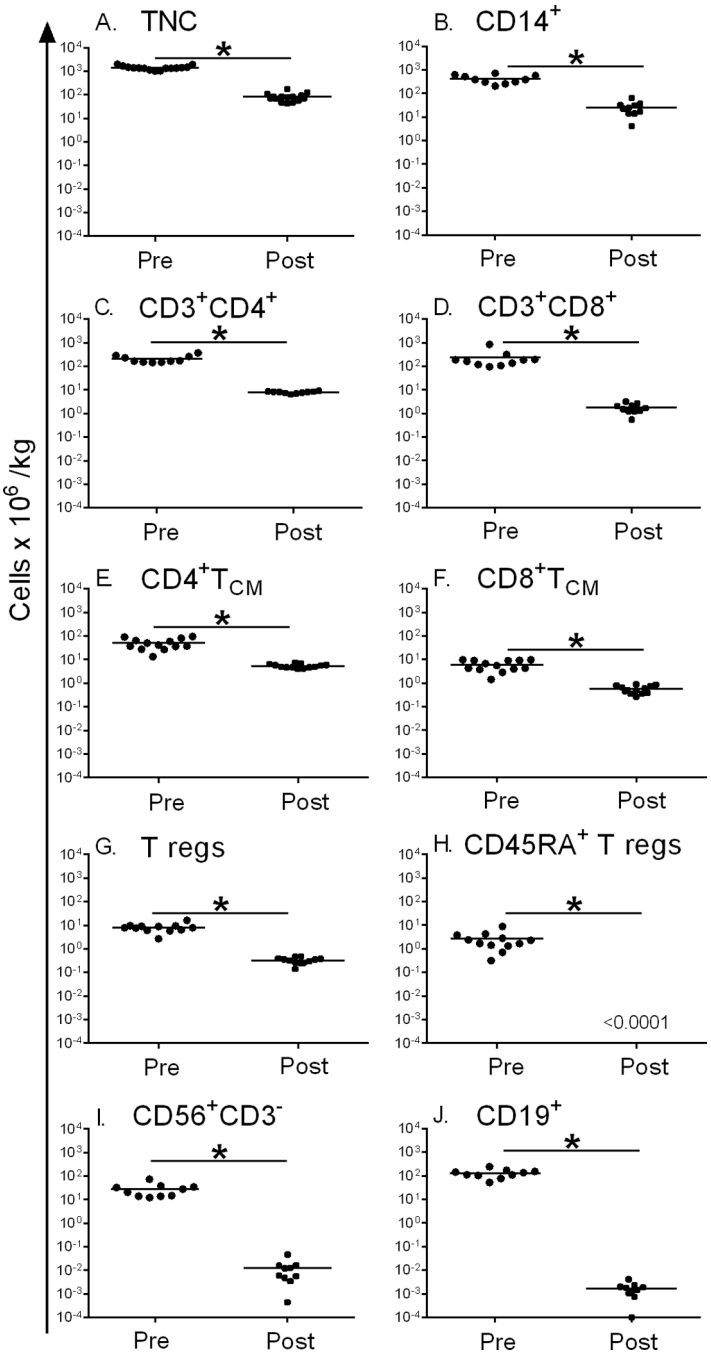

Figure 4. Cell composition of G-PBSC before and after CD45RA-depletion

Enumeration of cell content of G-PBSC before (circles) and after (squares) CD45RA-depletion. A) Total nucleated cells B) $CD14^+$ monocytes C) $CD3^+$ $CD4^+$ T cells D) $CD3^+$ $CD8^+$ T cells E) $CD4^+$ T_{CM} ($CD3^+CD4^+CD45RO^+$ $CD45RA^-CCR7^+$ $CD27^+$ $CD28^+$) F) $CD8^+$ T_{CM} ($CD3^+CD8^+CD45RO^+$ $CD45RA^-CCR7^+$ $CD27^+CD28^+$) G) T regulatory cells ($CD3^+$ $CD4^+$ $CD25^+$ $FOXP3^+CD45RA^{+/-}$) H) $CD45RA^+$ T regulatory cells ($CD3^+CD4^+CD25^+FOXP3^+$ $CD45RA^+$) I) $CD56^+CD3^-$ NK cells J) $CD19^+$ B cells. * indicates $P<0.05$ (Student's paired t test)

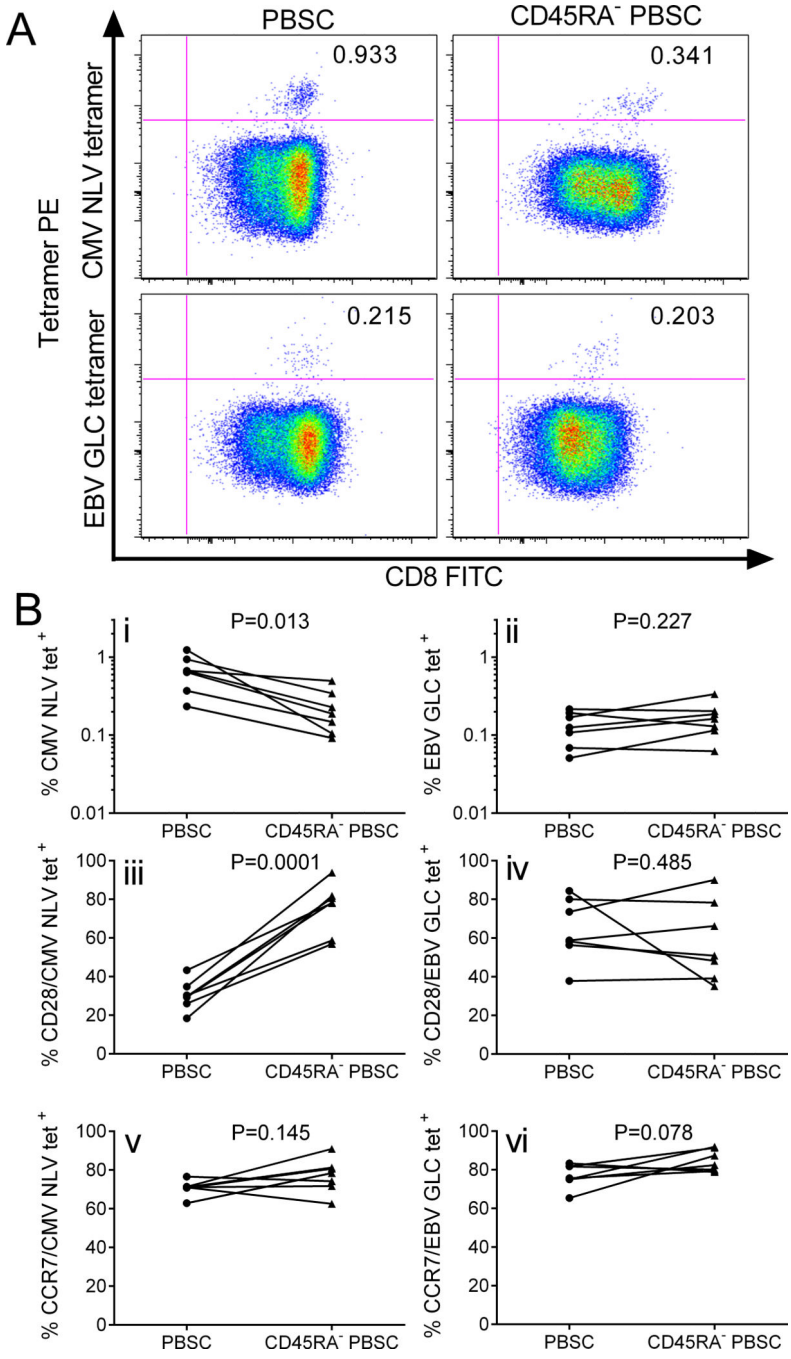

Figure 5. Virus-specific T cells in G-PBSC before and after CD45RA-depletion

A) Flow cytometry plots showing MHC tetramer staining for viral epitopes (CMV pp65 NLVPMVATV and EBV BMLF1 GLCTLVAML) of $CD8^+$ T cells enriched from G-PBSC and CD45RA-depleted PBSC from a representative HLA-$A2^+$ CMV^+ EBV^+ donor. B) Tetramer evaluation of G-PBSC and CD45RA-depleted PBSC from 7 HLA-$A2^+$ CMV^+ EBV^+ donors (i) CMV NLV specific T cells and (ii) EBV GLC specific T cells as a proportion of $CD8^+$ T cells; CD28 expression on (iii) CMV NLV $CD8^+$ and (iv) EBV GLC

$CD8^+$ T cells; CCR7 expression on (v) CMV NLV $CD8^+$ and (vi) EBV GLC $CD8^+$ T cells. Analyzed by Student's paired t test.

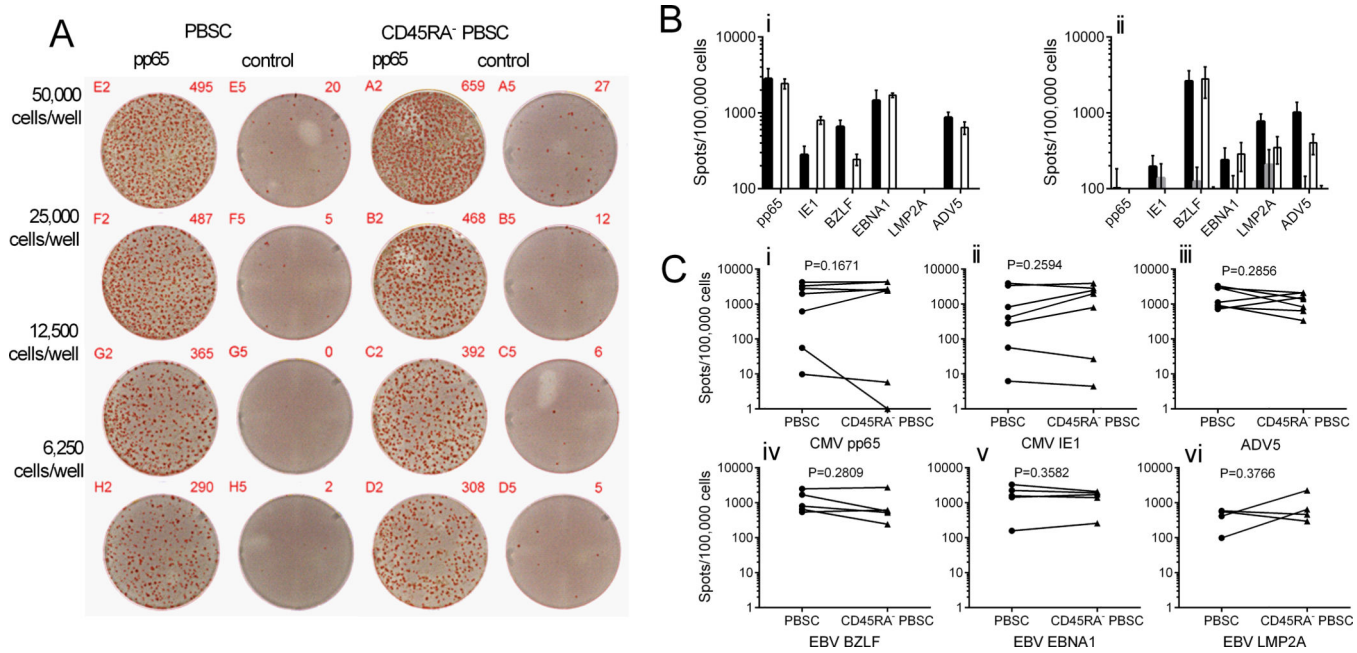

Figure 6. ELISpot assays evaluating pathogen-specific IFNγ secretion by T cells after peptide stimulation of G-PBSC and CD45RA$^+$-depleted G-PBSC

A) Representative IFN-γ ELISpot showing response of T cells from G-PBSC and CD45RA-depleted G-PBSC to pp65 and control (NYBR1) peptides. The figure shows one of three replicate wells for each cell concentration for each condition. B) IFN-γ ELISpot assay of T cells derived from G-PBSC and CD45RA$^+$-depleted G-PBSC from a CMV$^+$ donor (i) and a CMV$^-$ donor(ii) to CMV pp65, CMV IE1, EBV BZLF, EBV EBNA1, EBV LMP2A or adenovirus 15 mer peptide pools. Shown is the mean and standard deviation of the spot frequency in response to the viral or control peptide stimulation (PBSC + viral peptide = black, PBSC + control = dark grey, CD45RA-depleted PBSC + viral peptide= white, CD45RA-depleted+control=light grey C) IFN-γ response in donor PBSC (circles) and corresponding CD45RA-depleted PBSC (triangles): Responses to CMV pp65 (i) and IE-1 (ii) peptides in CMV seropositive donors (upper 5) and CMV seronegative donors (lower 2), adenovirus (iii), EBV BZLF (iv), EBNA-1 (v) and LMP2A (vi). Responses to control peptide are subtracted from the virus-specific response. Spot frequencies of <100/100,000 (<0.1%) are considered negative. Analyzed by Student's paired t test.

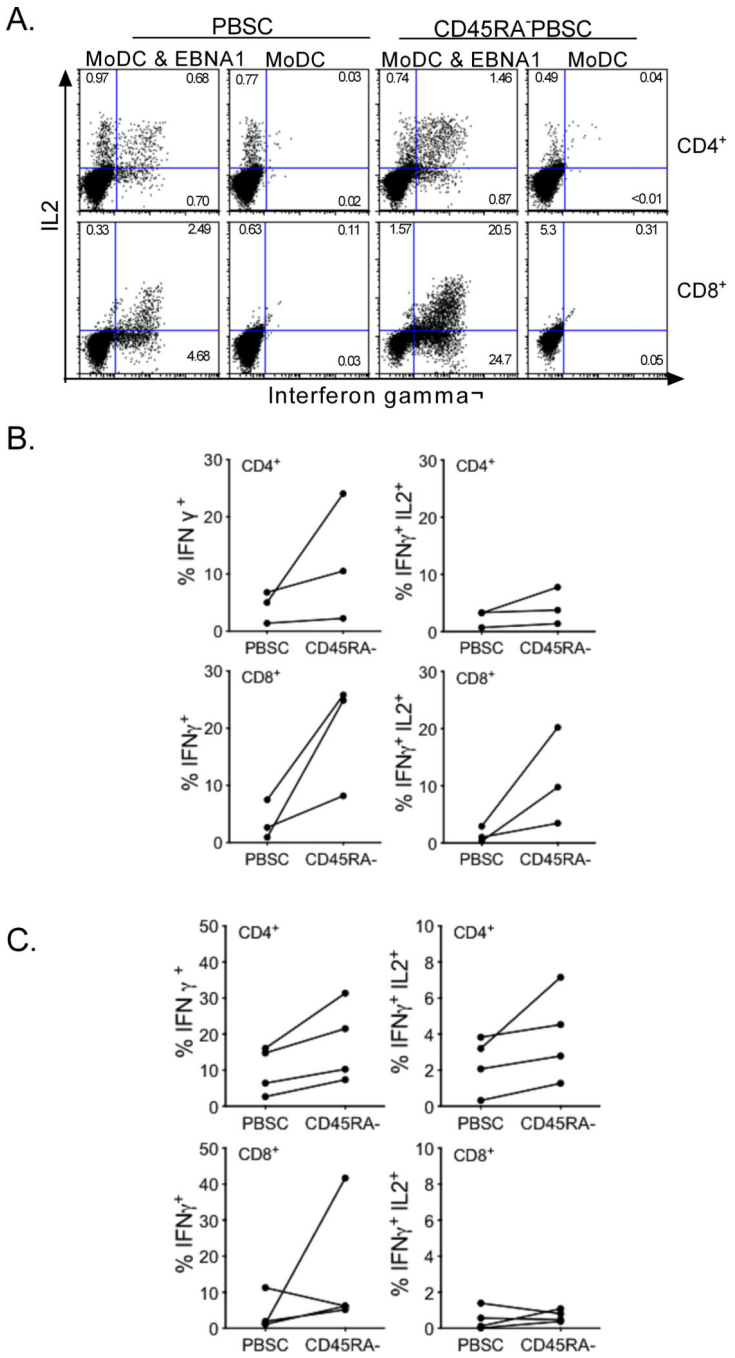

Figure 7. Intracellular cytokine flow cytometry to evaluate virus-specific T cells derived from PBSC and CD45RA-depleted PBSC

A) IFNγ and IL2 secretion by $CD4^+$ or $CD8^+$ T cells expanded from G-PBSC or $CD45RA^+$-depleted G-PBSC following re-stimulation with EBNA1 peptide or moDC alone B &C) Frequency of $CD4^+$ and $CD8^+$ T cells from G-PBSC or CD45RA-depleted G-PBSC from representative donors that produce IFNg or both IFNg and IL-2 after restimulation with B) EBNA-1 and C) pp65 peptides. The frequency of T cells responding to the negative control is subtracted from the data shown in B) and C).

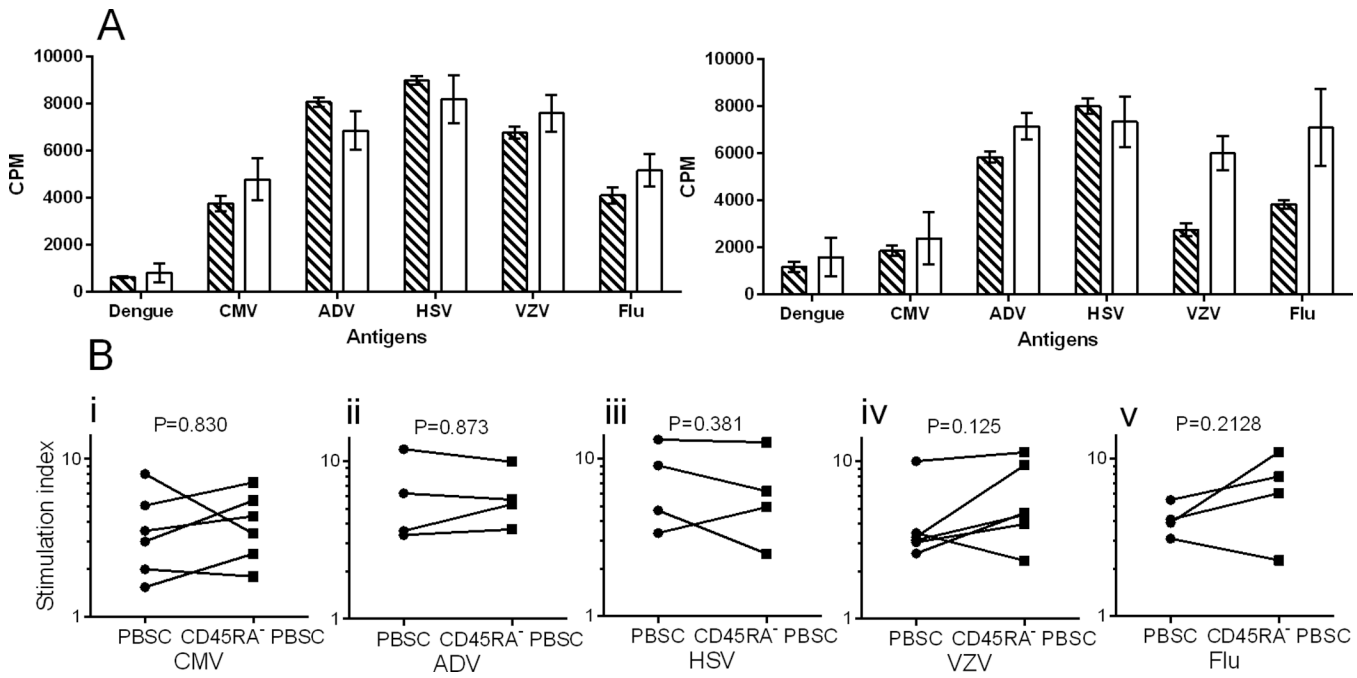

Figure 8. Lymphoproliferation assays to evaluate CD4$^+$ T cell responses to opportunistic pathogens

A) Proliferation of CD4$^+$ T cells enriched from G-PBSC (striped) and CD45RA$^+$-depleted G-PBSC (white) from representative CMV$^+$ (left) and CMV$^-$ (right) donors after stimulation with protein antigen preparations from dengue (negative control), CMV, adenovirus, HSV, VZV and influenza A viruses. Shown is the mean and standard deviation. B) Proliferation of CD4-enriched PBSC (circles) and CD45RA-depleted CD4-enriched PBSC (squares) in response to antigen stimulation with CMV (i), ADV (ii), HSV (iii), VZV (iv), and influenza. The stimulation index (SI) shows proliferation relative to negative control wells. A SI <3 is considered negative. Analyzed by Student's paired t test.

Table 1

	Starting G-PBSC (cells × 10^6/kg) (median, range)	CD45RA depleted G-PBSC (cells × 10^6/kg) (median, range)	Log depletion
Total nucleated cells	1369 (1031–1926)	80.85 (43–171)	1.23
$CD3^+$ T cells	382 (257–725)	9.99 (9.94–10.03)	1.58
$CD3^+T_N$ cells	186 (86.5–570)	0.0036 (0.0009–0.0078)	4.71
$CD3^+T_M$ cells	160.4 (75.7–274)	9.99 (9.94–10.03)	1.20
$CD3^+CD8^+$ T cells	174 (95.5–854)	1.62 (0.55–3.18)	2.03
$CD3^+CD4^+$ T cells	170 (145–369)	8.11 (6.5–9.38)	1.32
$CD3^+CD8^+$ T_{CM} cells ($CCR7^+CD27^+CD28^+$)	5.64 (1.43–9.84)	0.55 (0.266–0.89)	1.01
$CD3^+CD4^+$ T_{CM} cells ($CCR7^+CD27^+CD28^+$)	41.7 (13.5–96.3)	4.98(4.00–7.58)	0.92
$CD3^+CD4^+$ $CD25^+FOXP3^+$Tregs	7.88 (2.69–1.63)	0.337 (0.142–0.486)	1.37
$CD3^+CD4^+$ $CD25^+FOXP3^+CD45RA^+$Tregs	1.68 (0.319–4.32)	<0.0001	>4
$CD3^-CD56^+$NK cells	24.5 (12.3–74.6)	0.009 (0.0004–0.0462)	3.43
$CD19^+$ B cells	124 (52.9–244)	0.00164 (0.0001–0.004)	4.88
$CD14^+$ monocytes	390 (207–714)	23.9 (4.2–63.4)	1.21